Drift Characteristics of Sea-Bird Dissolved Oxygen Optode Sensors

ALICE S. REN,[a] DANIEL L. RUDNICK,[b] AND ALISTAIR TWOMBLY[b]

[a] *Woods Hole Oceanographic Institution, Woods Hole, Massachusetts*
[b] *Scripps Institution of Oceanography, La Jolla, California*

(Manuscript received 4 September 2022, in final form 5 October 2023, accepted 23 October 2023)

ABSTRACT: The Sea-Bird 63 dissolved oxygen optode sensors used on various oceanographic platforms are known to drift over time. Corrections for drift are necessary for accurate dissolved oxygen measurements on the time scale of months to years. Here, drift on 14 Sea-Bird 63 dissolved oxygen optode sensors deployed on Spray underwater gliders over 5 years is described. The gliders with oxygen sensors were deployed regularly for 100-day missions as part of the California Underwater Glider Network (CUGN). A laboratory two-point calibration was performed on the oxygen sensor before and after glider deployment. Sensor drift during 100-day deployments was larger than during 100-day storage periods. Sensor behavior is modeled with a gain that asymptotically approaches 1.090 ± 0.005 with an *e*-folding time scale of 3.70 ± 0.361 years. At zero oxygen concentration, the sensor consistently reads around 3 μmol kg^{-1}; a negative offset term is used in addition to the gain to correct the sensor oxygen. The correction procedure removes the error due to long time drift, one of the major sources of error, with an uncertainty of 0.5% (0.9% including outliers) or 0.5 μmol kg^{-1} depending on concentration, which improves the accuracy of the Sea-Bird 63 although uncertainty from other sources of error including the initial factory calibration and the sensor response time remain. Suggested procedures for implementing a two-point calibration procedure in the laboratory are discussed. Calibrations must be considered starting 6 months after initial factory calibration to keep error from sensor time drift under 1%.

SIGNIFICANCE STATEMENT: Dissolved oxygen measurements are widely used in oceanography. The optode sensors used to measure dissolved oxygen are known to drift over time. Here, the characteristics of drift for the oxygen optode sensor from Sea-Bird Scientific are described using a two-point calibration at zero and full saturation. The calibration procedure can be applied to oxygen optode sensors deployed on a variety of platforms when it is impractical to complete a multipoint calibration.

KEYWORDS: Oceanic chemistry; Data quality control; In situ oceanic observations; Instrumentation/sensors

1. Introduction

The California Underwater Glider Network (CUGN) is a long-term monitoring glider network started in 2007 with currently over 14 years of temperature, salinity, and velocity data on regularly sampled transects in the California Current System (CCS). Since 2017, gliders have carried a Sea-Bird 63 (SBE63) optode dissolved oxygen sensor as part of their payload. Since dissolved oxygen sensors are known to drift after calibration, it is desirable to have a correction procedure in place while collecting observations. Sensors read increasingly lower oxygen values over time, requiring an upward adjustment of values to correct the sensor data or a new multipoint calibration of the sensor. For the SBE63, Sea-Bird performs a 24-point calibration with four oxygen values and six temperatures at the time of manufacture, which sets the sensor's initial accuracy (Sea-Bird 2017). Sending an optode sensor to Sea-Bird to repeat a multipoint calibration before and after individual 3-month glider deployments is impractical, and a correction procedure that can be performed in an oceanographic laboratory is necessary. We present a two-point calibration procedure to correct oxygen optode sensor data and measurements of instrument drift over 5 years on 14 SBE63 optode sensors used on gliders. A two-point calibration has been shown effective on studies of mainly Aanderaa optodes, as the majority of drift is proportional with oxygen concentration and a small adjustment is needed at very low oxygen concentrations (Bittig et al. 2018a; Johnson et al. 2015). The novelty of this study is having many measurements of drift during 3–4 month deployments and during 3–4 months of storage. Our record of corrections of SBE63 sensors adds to a growing literature of assessments of oxygen sensors including Aanderaa optodes (Bittig and Körtzinger 2015; Bittig et al. 2018a; Bushinsky et al. 2016; D'Asaro and McNeil 2013; Johnson et al. 2015; Körtzinger et al. 2005). The suggested procedure removes the error due to long time drift with an uncertainty of the larger of 0.5% (0.9% including outliers) or 0.5 μmol kg^{-1} and is necessary for any dissolved oxygen sensor in use more than 6 months after calibration.

The SBE63 uses the same principle as the Aanderaa optode, and the two brands of sensors use the organometallic molecule platinum porphyrin as the luminophore and the same material for the sensor membrane (Bittig et al. 2018a), though details in the engineering or manufacturing process may differ. The sensor luminophore is excited with blue light and subsequently releases energy through fluorescence. An excited molecule can return to its original energy state in one of three ways: 1) it can emit a photon in a radiative process of fluorescence or phosphorescence, 2) it can release energy through nonradiative means collectively termed static quenching, and 3) it can collide with

Corresponding author: Alice S. Ren, alice.ren@whoi.edu

DOI: 10.1175/JTECH-D-22-0103.1

other molecules and transfer energy in a nonradiative process called dynamic quenching. Dynamic quenching occurs for platinum porphyrin in the presence of oxygen. Given excited molecules $[A^*]$, lowered energy state molecules $[A]$, photons of light $h\nu$ and quenching molecules $[Q]$, processes 1–3 occur at rates k_1, k_2, and k_q assumed to be constants (Demas et al. 1999):

$$1)\ [A^*] \rightarrow [A] + h\nu \qquad \text{Fluorescence} \qquad k_1, \quad (1)$$

$$2)\ [A^*] \rightarrow [A] \qquad \text{Static quenching} \qquad k_2, \quad (2)$$

$$3)\ [A^*] + [Q] \rightarrow [A] + [Q] \qquad \text{Dynamic quenching} \qquad k_q. \quad (3)$$

In this paper, the $[Q]$ is the concentration of oxygen, and k_q is the bimolecular quenching constant for oxygen. Because oxygen gas behavior is near ideal, the oxygen activity is interchangeable with oxygen concentration. For natural rate of decay without dynamic quenching, the rate of change is

$$\frac{d[A^*]}{dt} = -k_1[A^*] - k_2[A^*] = -(k_1 + k_2)[A^*]. \quad (4)$$

With dynamic quenching, the rate of change is

$$\frac{d[A^*]}{dt} = -(k_1 + k_2 + k_q[Q])[A^*], \quad (5)$$

where quenching increases as the concentration of the quenching molecule increases. The time scale of decay, or the fluorescence lifetime for natural decay L_0 is

$$L_0 = \frac{1}{k_1 + k_2}, \quad (6)$$

and with quenching the fluorescence lifetime L_q is

$$L_q = \frac{1}{k_1 + k_2 + k_q[Q]}. \quad (7)$$

The ratio of the original decay time scale to the decay time scale with quenching is

$$\frac{L_0}{L_q} = 1 + k_q L_0[Q]. \quad (8)$$

Equation (8) is also known as the Stern–Volmer equation when written with the constant k_{sv}:

$$\frac{L_0}{L_q} = 1 + k_{sv}[Q]. \quad (9)$$

The concentration of oxygen, $[Q] = [O_2]$, causes a decreased fluorescence lifetime of the platinum porphyrin molecule in the SBE63 optode theoretically at the rate proportional to k_{sv}. Thus, deviations in fluorescence from an oxygenated to nonoxygenated environment can be measured and converted into the concentration of dissolved oxygen present.

Given the bimolecular quenching constant k_q at a given temperature the Stern–Volmer equation should be linear. However, in optodes k_{sv} changes its value for high $[O_2]$, which suggests that some of the luminophore in the membrane is inaccessible to oxygen in high $[O_2]$ environments (Johnson et al. 2015), so in optodes an empirical model is used. Calibration coefficients are developed for each sensor that span a range of conditions in temperature and dissolved oxygen concentration. The relationship between phase delay of a sinusoidally modulated excitation and $[O_2]$ is more reliable than direct measurements of the fluorescence lifetime, and the phase delay relationship is used. Phase delay and fluorescence lifetime are related by

$$\tan\phi = 2\pi f L, \quad (10)$$

where f is the modulated frequency of the excitation light source in Hz, ϕ is the phase delay, and L is a general decay time scale or fluorescence lifetime (Demas et al. 1999). The SBE63 empirical model is based on work by Uchida et al. (2008) and relates oxygen concentration to phase delay:

$$[O_2] = \left[\frac{(a_0 + a_1 T + a_2 V^2)}{(b_0 + b_1 V)} - 1\right][K_{sv}]^{-1}[S_{corr}][P_{corr}], \quad (11)$$

where V is the phase delay (volts), T is temperature (°C), a_0, a_1, a_2, b_0, and b_1 are calibration coefficients, and K_{sv} is determined by calibration coefficients (Sea-Bird 2017). The dissolved oxygen concentration, $[O_2]$, is reported (mL L^{-1}). Corrections to account for the salinity of seawater S_{corr} and the pressure P_{corr} are also included (Sea-Bird 2017).

The concern in this paper is the time drift of the coefficients in the model relating $[O_2]$ and the phase delay ϕ [Eq. (11)]. The drift has been documented to change the measured oxygen concentration on the order of 10% on the time scale of years (Bittig and Körtzinger 2015; Bittig et al. 2018a). The temporal drift can be corrected with a gain and offset calculated from a two-point calibration with an $[O_2]$ observation at full saturation and zero saturation (Bittig et al. 2018a),

$$[O_2]_{corr} = G[O_2]_{raw} + Z, \quad (12)$$

where G is the gain, Z is the offset, and the subscripts indicate the raw or corrected (corr) dissolved oxygen concentration values from the optode sensor. The recommended best practice is to use a two-point calibration when a multipoint calibration is impractical or between periodic multipoint sensor calibrations (Bittig et al. 2018a). A multipoint calibration would span a range of temperatures and dissolved oxygen concentrations and would generate new coefficients for Eq. (11).

While optodes have been used on gliders before (Alkire et al. 2014; Damerell et al. 2016; Haskell et al. 2019; Howatt et al. 2018; Hull et al. 2021; Nicholson et al. 2008; Nicholson and Feen 2017; Nicholson et al. 2015; Pelland et al. 2018; Pietri and Karstensen 2018; Pizarro et al. 2016; Schütte et al. 2016), this study presents data from optodes used regularly as part of a monitoring program for the CCS. The SBE63s are evaluated roughly every 4 months. The intervals between evaluations are

either while the glider is deployed in the ocean or when the glider is on land in the laboratory being prepared for the next deployment. Based on the literature, it is unclear whether there is a difference in the drift rate of optodes while stored or while deployed in the ocean, though studies suggest that the drift that occurs during deployment is smaller than the drift during storage (Bittig et al. 2018a). One goal for this study is to compare drift rates while deployed and while in storage, and the novelty of the study is that sensors are calibrated repeatedly after short deployments and short periods of storage.

Because of the glider deployment schedule in CUGN and because any protocol implemented would be performed with high repetition, the measurements must be simple. The resulting two-point calibration should be achievable by a wide range of users. The full saturation reading of the optode is done with an in-air method and an in-water method, and the results are compared. The reading of the optode at zero oxygen is generally more challenging to set up. We choose a chemical means of creating a zero-oxygen environment with a sodium sulfite solution. We focus on the laboratory procedures, but also consider calibration by comparison of the glider values to collocated bottle samples of dissolved oxygen from California Cooperative Oceanic Fisheries Investigations (CalCOFI) cruises. Overall, the drift of the SBE63s over 5 years is described, whether stored in air or deployed in the ocean, and suggestions for procedures to correct for dissolved oxygen drift are provided.

2. Materials and methods

The SBE63 optodes are deployed on underwater gliders, vehicles that profile vertically using changes in buoyancy and move horizontally using wings and through internally shifting their center of mass (Rudnick 2016). We use Spray gliders (Sherman et al. 2001) operating as part of CUGN in the central and southern CCS. The gliders provide continuous coverage on 300–500 km onshore–offshore transects; a single glider mission is around 100 days at which point the glider is recovered and another glider is deployed in its place (Rudnick et al. 2017). Glider dives are up to 500 m depth and individual dives are 3 h and 3 km apart. A pumped flow system ensures reliable flow through sensors on the glider which include a conductivity–temperature–depth (CTD) sensor, a fluorometer, and a dissolved oxygen SBE63 optode sensor.

The routine operation of gliders in CUGN involves a roughly 100-day mission followed by a roughly 100-day storage period during which the glider is serviced. Sensor drift is calculated before and after glider missions. Evidence suggests that optode drift can be detected within weeks of calibration (Bittig et al. 2018a; Bushinsky et al. 2016), so measurements were collected within 1 month of glider deployment or recovery, with the vast majority of measurements occurring within 2 weeks. Readings outside the 1-month period are treated as "test" drift observations and included in some of the subsequent analysis. The reading before deployment is the "pre" deployment observation, and the reading after deployment is the "post" deployment observation.

The environmental conditions and modes of operation of the optode sensors while deployed and on land are as follows. While the Spray glider is deployed in the California Current System as part of CUGN, it makes a profile every 3 h. The optode makes a measurement every 8 s while profiling from 500 m depth to the surface at around 0.1 m s^{-1}, so 625 measurements are in each profile. For a 100-day mission, roughly 500 000 samples are taken with the optode. The temperature ranges from 5° to 19°C in the mean annual cycle in the region and depths covered (Rudnick et al. 2017). The SBE63 is stored connected to the glider during its 100 days out of the water, except to do measurements for the dissolved oxygen correction, when it is removed. When installed, the SBE63 is connected to the plumbing of the flow-through system that runs through the sensors in the rear bay (Fig. 1). While installed on the glider in the laboratory, a CTD check in a water bath and ballasting in a test tank are performed, and for these checks the dissolved oxygen optode sensor is submerged in water. Otherwise, gliders are stored dry, indoors, in a science and engineering laboratory. The humidity of the dissolved oxygen sensor while it is connected to the plumbing is not recorded.

The measurements for dissolved oxygen correction were performed at room temperature. San Diego has a mild seasonal temperature range, and the temperatures in the laboratory are controlled although not very strictly due to the mild climate.

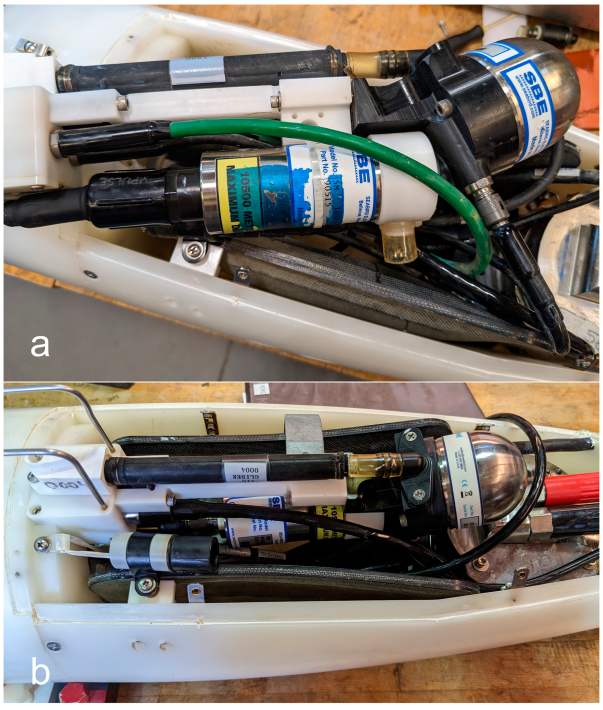

FIG. 1. Setup of the SBE63 optode dissolved oxygen sensor on the Spray underwater glider. The SBE63 is connected to a plumbed system wherein seawater is pumped through the instruments. The SBE63 sits behind the seawater intake and the CTD. After exiting the dissolved oxygen sensor, the water flows through the pump and the fluorometer. (a) Detailed profile view of the CTD, oxygen optode, and pump when disconnected from the bulkhead and the fluorometer. (b) Plan view of the SBE63 installed in the rear sensor bay of the Spray underwater glider.

The data collected here were taken at a mean temperature of 21.836°C with a standard deviation of 2.333°C (n = 291). The minimum measurement temperature was 15.840°C and maximum measurement temperature was 28.047°C, which should roughly approximate the range of temperature the sensors experience throughout a year while in storage. The calibration readings were performed in stable temperature conditions. The standard deviation of the temperature change within each 5-min measurement period for the calibrations, averaged among all measurements, was 0.013°C (n = 291).

a. Measurements of optodes at full saturation

The two-point calibration is determined with two assessments of the optode dissolved oxygen concentration against a known standard. One of the assessments is at full saturation, or the amount of dissolved oxygen found in water at equilibrium with the atmosphere. The full saturation concentration of dissolved oxygen is calculated with Garcia and Gordon (1992) Eq. (8) using coefficients fit to data from Benson and Krause (1984). The Eq. (8) in Garcia and Gordon (1992) is well-known to have a typo, and the corrected equation is reproduced here for clarity:

$$[O_2^*(T, S)] = e^{A_0 + A_1 T_s + A_2 T_s^2 + A_3 T_s^3 + A_4 T_s^4 + A_5 T_s^5 + B_0 S + S\,(B_1 T_s + B_2 T_s^2 + B_3 T_s^3) + C_0 S^2}, \quad (13)$$

where $[O_2^*(T, S)]$ is the full saturation concentration of dissolved oxygen at 1 atm (mL L^{-1}), T_s is a scaled temperature defined in Garcia and Gordon (1992), S is the salinity, and the remaining variables are constants defined in Garcia and Gordon (1992). The scaled temperature T_s is

$$T_s = \ln\left(\frac{298.15 - T}{273.15 + T}\right), \quad (14)$$

where T is the temperature (°C). In addition, the equation is corrected to account for differences in atmospheric pressure using a slightly modified version of the pressure correction term suggested in Benson and Krause (1984) Eq. (24):

$$P_f = \frac{(P_a - pH_2O \cdot R_h)(P_r - \theta_0 P_a)}{(P_r - pH_2O \cdot R_h)(P_r - \theta_0 P_r)}, \quad (15)$$

where P_f is the correction term, P_a is the measured atmospheric pressure (atm), P_r is a reference pressure defined as 1 atm, pH_2O is the saturated water vapor pressure (atm), and θ_0 is the second virial coefficient of oxygen gas. The relative humidity of the atmosphere R_h is 1 when the optode is used in water but can be less than 1 when the optode is making a measurement in air. The saturated water vapor pressure is calculated using Eq. (10) in Weiss and Price (1980). The second virial coefficient is calculated using the empirical relationship in Benson and Krause (1984) Table 2. The terms containing the second virial coefficient at 0°C contribute a 0.01% correction factor at pressures from 0.95 to 1.05 atm. The remaining terms contribute a correction factor on the order of the pressure deviation from 1 atm. For example, at 18°C, 0 salinity, 0.98 atm, and 100% relative humidity, the correction with and without the virial coefficient terms is 0.98. The pressure correction suggested for oxygen measured on biogeochemical Argo floats is Eq. (13) without the virial coefficient terms (Bittig et al. 2018b). The concentration at full saturation of dissolved oxygen including the atmospheric pressure correction is

$$[O_2^*(T, S, P)] = [O_2^*(T, S)] \cdot P_f. \quad (16)$$

The full saturation concentration is compared to the concentration of dissolved oxygen measured by the SBE63, $[O_2]$, to calculate the saturation of dissolved oxygen:

$$\text{sat}(O_2) = \frac{[O_2]}{[O_2^*(T, S, P)]}, \quad (17)$$

where sat(O_2) is the oxygen saturation described as a ratio where a value of 1 is full saturation.

Full saturation conditions are achieved in water by using an air bubbler in a beaker of freshwater (Fig. 2). Seven hundred milliliters of water are used, which covers the SBE63 while in a 2000 mL glass beaker. The air bubbler is a type used in fish tanks and an aquarium stone is attached to the pump to generate small air bubbles. The measurement at full saturation is performed at room temperature. A room with stable temperature is needed to ensure that the water is at room temperature and that the water is not changing temperature during the readings for the full saturation endpoint. A beaker of 700 mL of water will usually equilibrate to room temperature within a few hours. The average of dissolved oxygen concentrations taken every 10 s for a 5-min period is used as one full saturation endpoint measurement. Full saturation conditions always exist in air, and the second method of a full saturation endpoint determination is to read the optode while exposed to air (Fig. 2b). The average of dissolved oxygen concentrations taken every 10 s for a 5-min period is used as one full saturation endpoint measurement.

The parameters recorded during both in-water and in-air full saturation readings include the atmospheric pressure, the temperature of the water or air, and the relative humidity. The atmospheric pressure is taken from a local weather station or a sensor at Scripps pier. The pressure reading from the sensor at Scripps pier is adjusted for the height of the glider laboratory from sea level, roughly 67 m. The temperature of the water or air is recorded by the SBE63. The relative humidity is estimated from a local weather station or a humidity sensor in the glider laboratory. The relative humidity is set to 1 for the in-water saturation reading. The salinity is zero in both full saturation methods.

b. Measurements of optodes at zero saturation

The second endpoint for the two-point calibration is an assessment of the optode at zero dissolved oxygen. Borrowing from a procedure outlined in an Aanderaa product manual

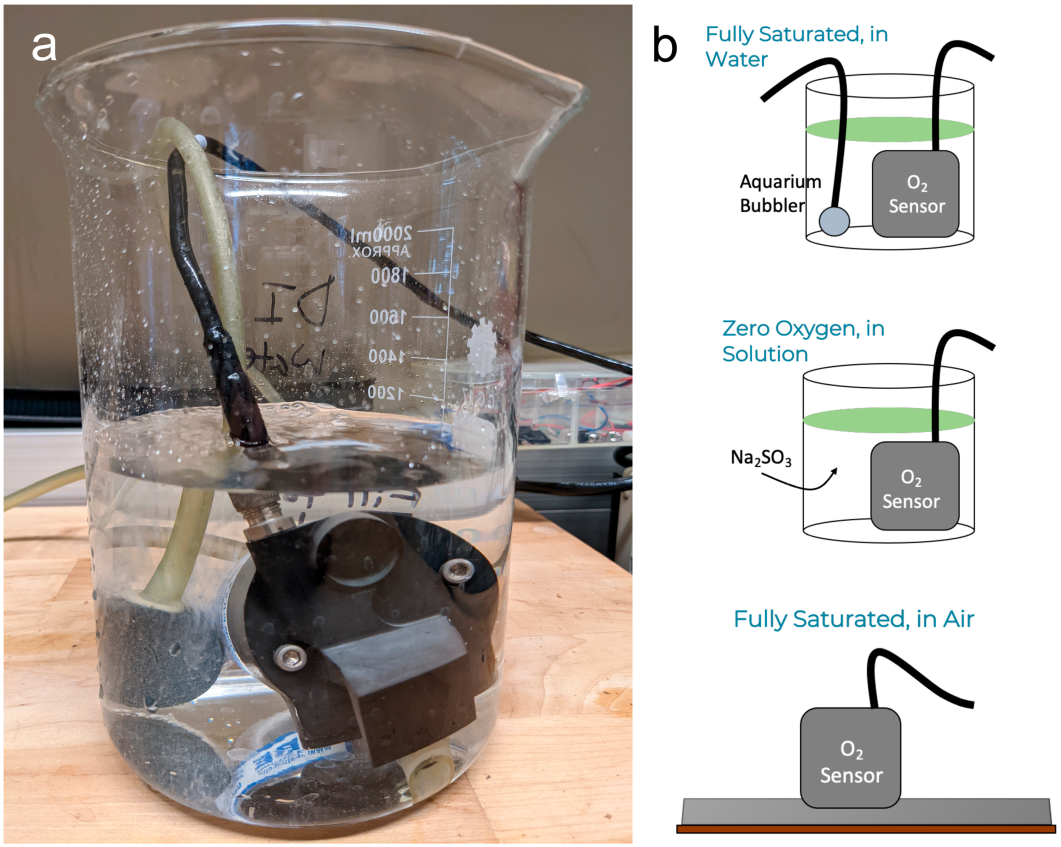

FIG. 2. Setup of the SBE63 optode dissolved oxygen sensor for measurements of full saturation and zero dissolved oxygen. The SBE63 is removed from the Spray underwater glider and connected directly to a computer via a communication cable. (a) The setup of full saturation conditions in water using an aquarium stone bubbler (blue). (b) Schematic representations of the three conditions: (top) full saturation in water, (middle) zero dissolved oxygen using a solution of sodium sulfite, and (bottom) full saturation in air.

(Aanderaa 2015), a solution of sodium sulfite was created, using 20–30 g of sodium sulfite (Na_2SO_3) and 700–800 mL of water in a 2000 mL glass beaker (Fig. 2b). The procedure uses more than the 10 g L^{-1} of sodium sulfite recommended by Aanderaa. The chemical reaction that strips the solution of dissolved oxygen is

$$2SO_3^{2-} + O_2 \rightarrow 2SO_4^{2-}, \tag{18}$$

where the sulfur is oxidized from 4+ to 6+ and the oxygen gas is reduced. In practice, the water is left at room temperature for a few hours to equilibrate its temperature. The sensor is left in the sodium sulfite solution for at least an hour before taking a reading at zero, which we hypothesize gives enough time for any oxygen gas introduced by the process of submerging the sensor to be stripped from the solution, including gas on the sensor or in the inflow or outflow cavity. The average dissolved oxygen concentration taken every 10 s for a 5-min period is used as a zero-endpoint measurement. Following being submerged in the sodium sulfite solution, the optode is rinsed in freshwater before being allowed to dry and being put back in storage. The temperature and atmospheric pressure are also recorded for the zero-oxygen endpoint, but only the concentration of dissolved oxygen is needed to calculate the gain and offset coefficients.

c. *Gain and offset calculation*

The measurements of oxygen saturation and oxygen concentration at the full saturation endpoint and oxygen concentration at the zero-oxygen endpoint allow calculation of the gain and offset. The measured concentration at zero, $[O_2]_z$, the measured concentration at full saturation, $[O_2]_f$, and the theoretical full saturation value, $[O_2^*(T, S, P)]$, are used:

$$G = \frac{[O_2^*(T, S, P)]}{[O_2]_f - [O_2]_z}, \tag{19}$$

$$Z = -G[O_2]_z. \tag{20}$$

The offset has the opposite sign of $[O_2]_z$ because it compensates for the observed dissolved oxygen concentration in the zero-oxygen environment.

The gain and offset laboratory coefficients were calculated beginning in November 2018, after some sensors had already

been deployed since December 2016. For many sensors, the first measurement of the gain and offset coefficients are one or two years after factory calibration at Sea-Bird.

d. Comparison of laboratory measurements to correction via opportunistic hydrographic measurements

CalCOFI bottle samples of dissolved oxygen determined by Winkler titration are used to obtain a gain correction for sensors on selected glider deployments. The glider transects in CUGN run along CalCOFI hydrographic lines, lines 66.7, 80.0, and 90.0. Lines 80.0 and 90.0 are sampled quarterly by CalCOFI ships. Dissolved oxygen from Winkler titrations of bottle samples from CalCOFI are compared to the nearest glider dive in time, horizontal distance, and isopycnal surface. Glider oxygen profiles are corrected for the slow response time of the optode sensor (Bittig et al. 2018a) by applying a lag of 24 s. Making comparisons on isopycnal surfaces minimizes the effect of heaving by internal waves or other processes. The comparison is limited to oxygen concentration above 1 mL L^{-1}, or 44 μmol kg^{-1} at seawater density of 1.025 kg L^{-1}. The precision of Winkler measurements is 0.005–0.010 mL L^{-1} (Culberson et al. 1991; Langdon 2010), or 0.22–0.44 μmol kg^{-1} at seawater density of 1.025 kg L^{-1}, so comparison of dissolved oxygen values close to zero is ineffective. Due to the oxygen minimum zone in the CCS, often values between 340 and 500 m deep are excluded. A weighted least squares fit between the CalCOFI cast and the glider profile is performed to determine a gain. Only a gain correction is applied since the fit emphasizes surface values and ignores values near zero oxygen concentration. The fit is weighted by the inverse of the variance of dissolved oxygen from nearby glider dives to account for horizontal variability of dissolved oxygen in the environment. The nearby glider dives are those within half of the horizontal distance between the glider dive and CalCOFI cast. The distance between adjacent CalCOFI stations is up to 74 km.

Hydrographic comparison of casts and glider dives are attempted for glider deployments between December 2016 and 2019. In the case when the comparison is in shallow, nearshore waters, the gain is not reported. Gain values of 1.1 or higher are discarded as unreliable estimates.

3. Results

a. Gain values over time

The evolution of the gain coefficient shows a nonlinear increase over time that is consistent among almost all the 14 SBE63 oxygen sensors. The gain coefficient as computed from the in-water saturation technique shows the clearest pattern of change over time (Fig. 3a). Eleven out of the 14 sensors appear to evolve similarly. At 2000 days or roughly five and a half years after calibration at Sea-Bird or factory calibration, five sensors have a gain of roughly 1.07. Six additional sensors lie on the curve from 0 to 2000 days. For the majority of sensors, in the first 1000 days the gain increases from 1 to 1.05, while in the second 1000 days, the gain increases from 1.05 to 1.07, demonstrating the nonlinearity of the drift over time. Sensors 632494 and 632495 are outliers with greater gain values than expected while sensor 630754 has a noticeably lower gain over time compared to the others. The gain is more precisely measured using the in-water method than the in-air method (Fig. 3b), which can be seen in the comparison of gain over time plots.

The rate of drift during deployment is larger than during storage. Rates of change of the gain calculated from the in-water method during deployment or during storage have mean values of 0.018 and 0.008 yr^{-1}, respectively (Fig. 4), with standard error of the mean of 0.004 for both deployment and storage rates. We performed a one-tailed unpaired t test with unequal variances to test whether the mean change in gain during deployment is larger than the mean change in gain during storage and obtained a p value of 0.06. The result is worth reporting although the p value is greater than the 0.05 threshold that is often used for significance, casting some doubt that the null hypothesis is appropriately rejected. Trends in the measurements of storage drift rate and deployment drift rate over time are not reported. Error in the full saturation reading can be amplified when calculating the change in gain over short time periods such as 60 days. The better representation of the drift over time is the assessment of 97 calculations of gain from the in-water full saturation method presented in Fig. 3a.

b. Offset values over time

The measurements in zero-oxygen (Fig. 5) were found to be consistently small over time. Sensors 630757, 630227, 630755, 630756, 630759, 632050, and 632309 read consistent zero values over time, around 0.05–0.06 mL L^{-1} or 2–3 μmol kg^{-1}. Six of the remaining sensors appear to have slightly increasing measurements at zero, increasing in value by 0.02–0.03 mL L^{-1} over 4 years. Bittig and Körtzinger (2015) found increasing values at zero over time of 2 μmol kg^{-1} or 0.04 mL L^{-1} over 3 years on an Aanderaa 4330F optode sensor. Certain batches of sensors may behave differently over time. Alternatively, it is possible that small differences in the experimental setup caused some of the differences in the measurements. All values at zero, $[O_2]_z$, were 0.1 mL L^{-1} or less, so long-term changes in the correction over time for most of the SBE63s in this study are due to steady changes in the gain, rather than changes in the concentration measured at zero oxygen. The standard deviation σ of the measurements at zero is 0.011 mL L^{-1} or 0.49 μmol kg^{-1} (Fig. 5). The mean offset of all two-point calibrations is −0.064 and the standard deviation of the offset is 0.011 mL L^{-1}, which we take as the uncertainty in the offset procedure. The uncertainty of 0.011 mL L^{-1} or 0.49 μmol kg^{-1} in freshwater is 0.2% of full saturation at 10°C, salinity of 32, and 1 atm.

c. Gain from hydrographic comparisons

For applications of optode sensors without laboratory calibrations, comparison with hydrographic profiles is often used to correct the dissolved oxygen data. Over time, the gain coefficient from comparison with CalCOFI hydrographic profiles increases, as found in the laboratory calibrations (Fig. 6). There are fewer gain coefficients from hydrographic comparison because only one coefficient can be calculated per deployment and because of cases when the ship and glider profiles were not close enough. There are a few potential outliers. The first gain estimate of sensor 630754 is below 1, which is lower than

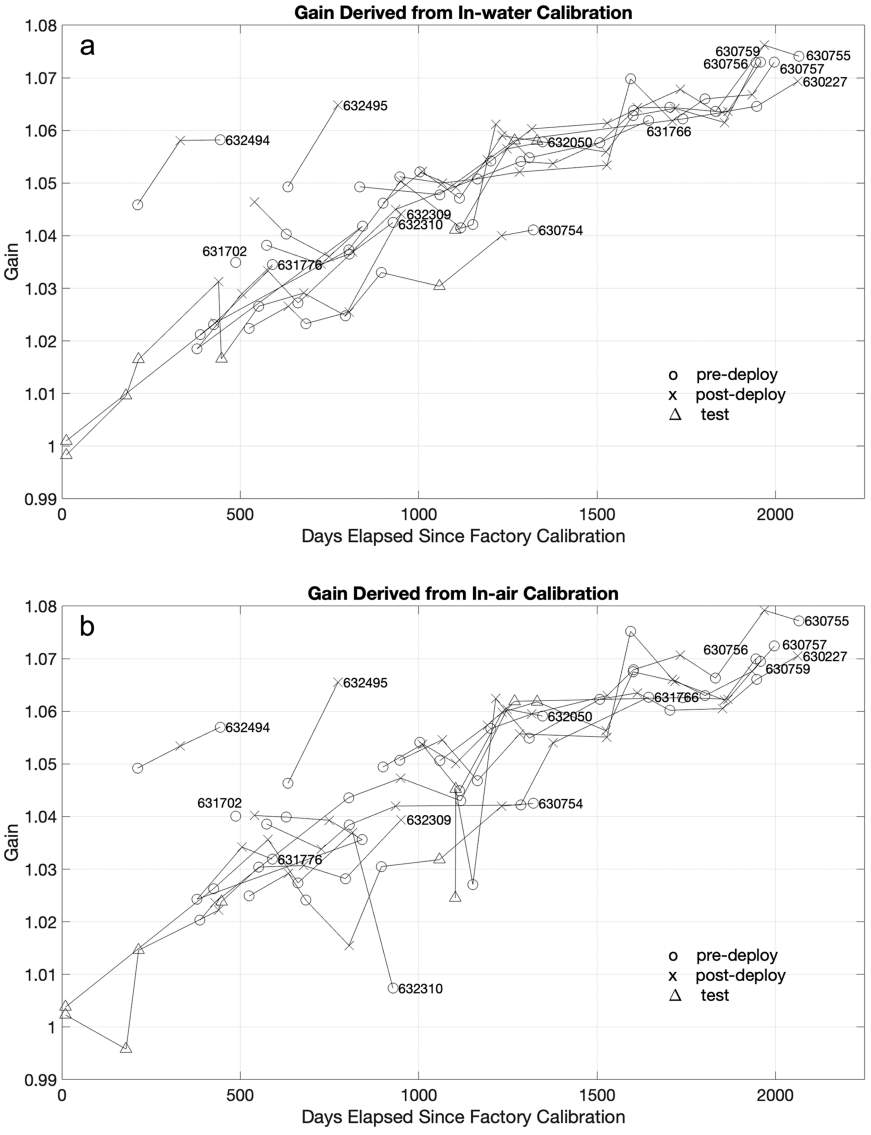

FIG. 3. Gain over time using (a) the in-water method and (b) the in-air method. The x axis is the number of days since the calibration at Sea-Bird, which calculates the full set of model coefficients for a range of temperature and oxygen concentrations. Gain values greater than one indicate that the SBE63 reads a lower concentration than present in the environment. The individual sensor gain values are plotted and labeled with the sensor serial number. Each gain value is marked by whether it was taken before a glider deployment, "predeploy" (◯), after a glider deployment, "postdeploy" (×), or at any other time, "test" (△).

expected. Sensor 630758 was lost at sea, and there is no comparable laboratory calibration time series. In contrast to a particular sensor being an outlier (Fig. 3), it appears that for any sensor there is a chance that the comparison is made using a bad match between hydrographic and glider profiles due to environmental variability.

d. Characterizing the drift over time

An exponential equation is fit to the gain evolution over time derived from the in-water full saturation method, and coefficients are found relating t, the days since calibration at Sea-Bird, and G_{mod}, the modeled gain value:

$$G_{\text{mod}} = 1 + M(1 - e^{-t/\tau}), \tag{21}$$

where M is the amplitude of the change in gain and τ is the e-folding scale or time scale of the function. Assuming this model allows for the estimation of the asymptotic gain and time scale, which may be helpful to characterize the sensor. The best fit model using least squares regression is $M = 0.090 \pm 0.005$ and $\tau = 1350 \pm 132$ days, which suggests that the maximum

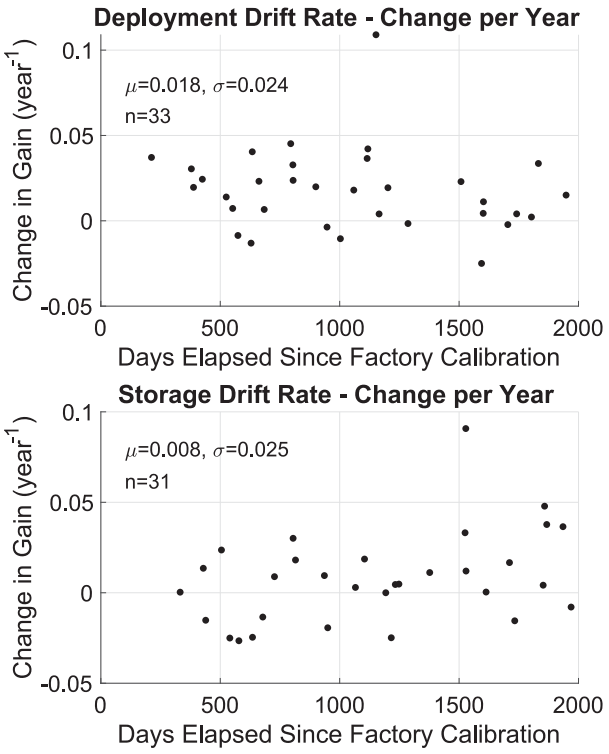

FIG. 4. Rates of change of the gain coefficient during storage and deployment (yr^{-1}) from the in-water full saturation method. The x coordinate of each data point is the days elapsed since calibration of the first of the pair of measurements used to calculate the rate of change. Mean values μ, standard deviations σ, and the number of data points n are displayed in the plots.

change in gain to be expected from the SBE63 sensors is 9% with an exponential time scale of 3.7 years (Fig. 7). The root-mean-square misfit between the data and the model is 0.0049. The one-standard-deviation error of M and τ are calculated from a bootstrap method using 100 000 synthetic datasets with standard deviation of 0.0049. The outliers of sensors 630754, 632494, and 632495 are not included in the fit because least squares regression is sensitive to extreme values; including the outliers, the root-mean-square misfit is 0.0090.

4. Discussion

The goals of the paper are to characterize the drift of SBE63s over 5 years, whether stored in air or deployed in the ocean, and to suggest procedures to correct for dissolved oxygen sensor drift. For the SBE63s on gliders, a correction procedure including an in-water full saturation measurement provides accurate results. The gain is modeled using an exponential equation that depends on the number of days since sensor factory calibration. Previous studies also found the drift evolution of Aanderra optodes to be nonlinear (Bittig et al. 2018a; D'Asaro and McNeil 2013). Bittig et al. (2018a) fit data from Aanderaa optodes with extensive usage applied during manufacturing, or a burn-in procedure, using an exponential with a time constant of 2.22 years and amplitude of 6% while Aanderaa optodes without the burn-in procedure had an amplitude of about 12%. In the results here, after 2 years since calibration, the gain is still found to increase at a significant rate. The coefficients of the exponential curve may be sensitive to how the SBE63 is stored or used. The time constant of 3.7 years and the amplitude of 9% are a good representation of the character of the 14 SBE63s which were treated in a nearly identical manner as part of CUGN.

A two-point calibration is less accurate than a multipoint calibration, but it has distinct advantages in ease of use. A primary benefit is that the two-point calibration can be done closer in time to deployment and recovery, thus determining whether drift occurred during storage or deployment. To compare between the multipoint and two-point calibrations, it would be necessary to perform both on a sensor and track changes over time, which was not done here with the SBE63. The 0.5% (0.9% including outliers) uncertainty of the gain coefficient is calculated using measurements at full saturation at room temperature, and although the dissolved oxygen concentration is known to drift proportionally with concentration such that one multiplicative gain constant can be used across all concentrations (Bittig et al. 2018a; Johnson et al. 2015), the error of the gain coefficient could vary with temperature and oxygen saturation, as has been shown when comparing Aanderaa optodes with corrected sensor coefficients from a multipoint calibration (coefficients a_0, a_1, a_2, b_0, b_1, and K_{sv} for Sea-Bird) to those with a two-point calibration (Bittig et al. 2018a).

With regard to the procedure, the in-air full saturation method is found to be inferior to the in-water full saturation method, and the opportunistic comparison with hydrographic casts is found to be the least effective method. The reasons for the in-air method to be unreliable are likely related to the sensor membrane and the protocol for the in-air measurement used here. The Aanderaa user manual suggests that the sensor membrane and luminophore are in a different state when completely dry and can have inaccurate dissolved oxygen readings. The sensor takes hours to become completely wet or dry, and spot measurements of a dry sensor in a wet environment have errors of 2% (Aanderaa 2015). Keeping a sensor humid for 12 h is equivalent to having a wet sensor (Aanderaa 2015). A procedure that could produce a reliable in-air measurement may be to submerge a sensor in freshwater for 3 or more hours and then perform a measurement in air, noting the relative humidity and using Eq. (15). One criticism of the aquarium pump method is that the introduction of bubbles can cause an environment oversaturated with dissolved oxygen. The in-water procedure here used bubbles created around 2 in. (~5 cm) from the surface within the glass beaker, which could have caused oversaturation of around 0.5%, comparable to the error in the two-point calibration which likely includes error from multiple sources. Consistent oversaturation would offset the modeled exponential curve vertically without changing its shape, and this error might be addressed by moving the bubbling stone to just below the water surface. In general, performing the calibration in the same media and phase as field calibrations may be preferred.

The comparison with hydrographic casts is impacted by the natural variability in the ocean on small scales and practical issues with matching casts with dives. In many instances, casts and dives are not found close enough in distance or time since

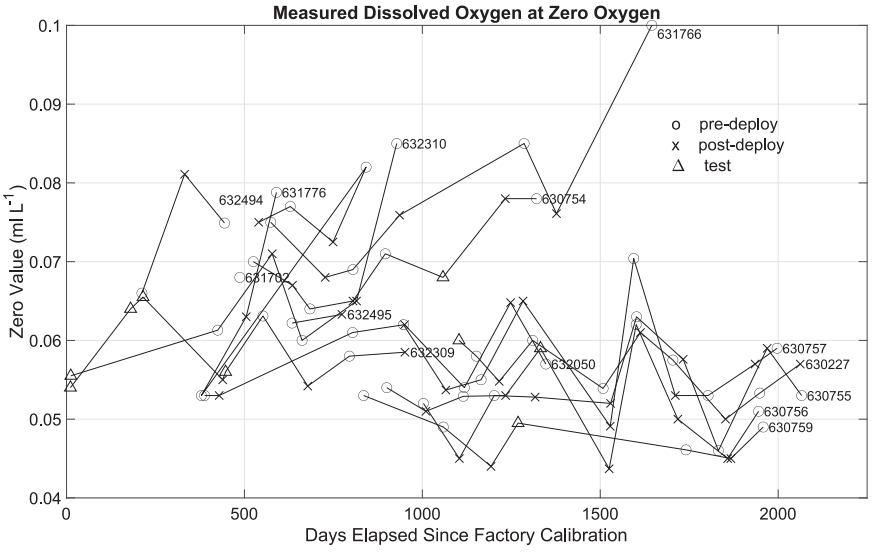

FIG. 5. Measured dissolved oxygen concentration in the zero-oxygen environment. The *x* axis is the number of days since the calibration at Sea-Bird, which calculates the full set of model coefficients for a range of temperature and oxygen concentrations. The individual measurements are plotted and labeled with the sensor serial number. Each measurement is marked by whether it was taken before a glider deployment, "predeploy" (◯), after a glider deployment, "postdeploy" (×), or any other time, "test" (△).

we are relying on opportunistic crossing of a ship with the glider track. When there is a matching dive and cast, horizontal variability in dissolved oxygen can cause an inaccurate gain estimate. In the CCS, there is an oxygen minimum zone, which impacts the accuracy of gain estimates using hydrography. The precision of Winkler titrations causes titrations near zero concentration to be less accurate, so the least squares comparison relies on observations in higher dissolved oxygen concentrations which have more variability. As a practical matter, coordination with a ship and obtaining Winkler titrations may be a significant task, and the laboratory correction may be easier to implement. Performing corrections

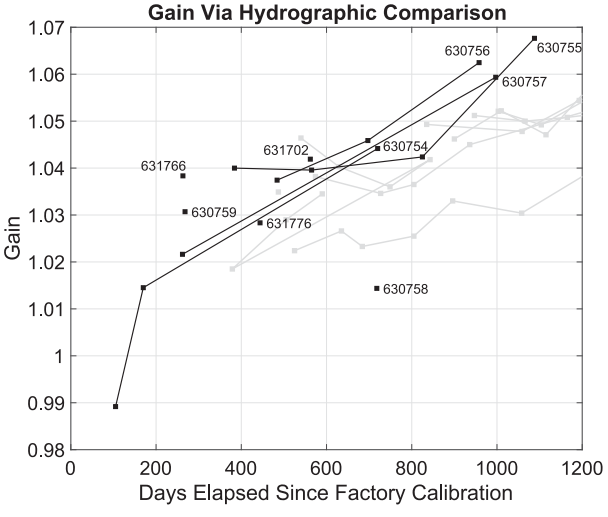

FIG. 6. Gain over time from comparison with CalCOFI dissolved oxygen samples. The individual sensor gain values are plotted and labeled with the sensor serial number (black). The gain coefficient determined by laboratory in-water calibration of the corresponding sensors is plotted in gray. The *x* axis is the number of days since the calibration at Sea-Bird, which calculates the full set of model coefficients for a range of temperature and oxygen concentrations.

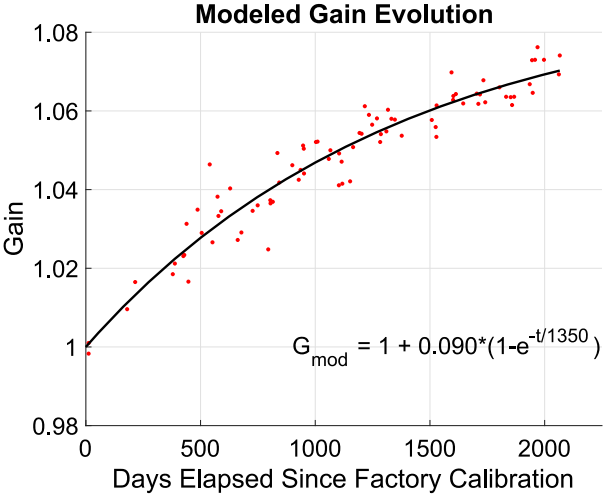

FIG. 7. Modeled gain evolution with time. The model (black line) is an exponential equation in *t*, the days elapsed since calibration at Sea-Bird and determines G_{mod}, the gain. The data contributing to the model are plotted in red dots and come from in-water calibrations of 11 SBE63 sensors (630754, 632494, and 632495 are excluded).

using laboratory procedures before deployment also allows for real-time corrected glider dissolved oxygen data. The combination of factors means that for the CUGN gliders, laboratory corrections are better than estimating gain from comparison with hydrography.

The measurements of the SBE63 at zero oxygen are of the same magnitude as in Bittig et al. (2018a), which lends support to their accuracy. However, we are not able to confidently describe trends over time in the concentration of dissolved oxygen measured at zero, while Bittig et al. (2018a) suggest a small increase over time. The data appear to have two clusters, with one set not showing any change over time and the other set showing slight increases. The coefficients of the Sea-Bird model are fit for a range of oxygen concentrations starting at near 1 mL L^{-1}, so it may be that the sensor model is not well fit to concentrations at or near zero concentration. Overall, in the zero-oxygen environment, a small nonzero concentration of dissolved oxygen on the SBE63s around 0.07 mL L^{-1} or 3 μmol kg^{-1} was consistently measured. It is worth noting that the initial accuracy of SBE63 sensors is ± 3 μmol kg^{-1} or $\pm 2\%$, whichever is larger depending on the oxygen concentration value (Sea-Bird 2017).

The drift during deployment is larger than the drift during storage in this study of 14 SBE63s used on the schedule of 100 days at sea and 100 days on land. This result is contrary to other studies that found faster drift during storage (Bittig et al. 2012, 2018a; D'Asaro and McNeil 2013). It is possible that 100 days of dry storage is not a long enough period for increased drift to occur or that the sensors were periodically wet during storage causing reduced drift. As part of the routine 100-day glider deployment schedule, the SBE63 is wet during the two-point calibration of the SBE63 and for the glider CTD check and glider ballasting. The outliers in the data experienced normal treatment except for one, sensor 632495, which was initially a spare. Spares are stored alone or on spare gliders and may spend 12 months or more in a dry environment. Drift of the sensor during usage is expected due to damage of the membrane from exposure to light needed to excite the luminophore. The Sea-Bird description of drift due to usage is a change of 1 μmol kg^{-1} per 100 000 measurements, calculated with respect to full saturation concentration at 20°C (Sea-Bird 2017). With 1 000 000 measurements per year, as would be typical of the Spray glider schedule in CUGN, the equivalent gain coefficient, without considering an offset coefficient, would be 1.0365 after 1 year. Our observed drift rate while deployed is less than expected from usage as estimated by the manufacturer.

While the results presented involved SBE63 optode oxygen sensors on gliders, optode oxygen sensors are used on floats including biogeochemical floats as part of the Argo program. The Biogeochemical-Argo (BGC-Argo) program has adopted the strategy of in-air calibrations of the optode sensor since the floats are not recovered after deployment. BGC-Argo floats aim to have a lifetime of 4 years (Bittig et al. 2019), comparable to a lifetime of an Argo float which can be 5 years or more (Roemmich et al. 2009). The float in-air procedure is approximately the same as the recommendation presented of in-air laboratory measurement of the SBE63 after the sensor foil is wet. A consideration for Argo float calibration is that the in-air measurement may be contaminated by measuring in part the surface ocean rather than only the atmosphere, a "carryover effect" (Bittig et al. 2018a) which is not an issue in the laboratory. Another source of error is that Argo in-air calibrations must determine the barometric pressure from a climatology, climate reanalysis, or operational model. The SBE63 drift over 5 years of use on gliders could be relevant to the time drift over the lifetime of a deployed float although differences may exist due to the sampling rate or environmental condition of the optode sensors on different platforms. Further research could track optode oxygen sensor time drift on BGC-Argo floats. As suggested by the results from the SBE63 used on gliders, an exponential correction over the lifetime of the float may be appropriate for optode sensors deployed for 4 years.

5. Conclusions

Through tracking 14 SBE63 dissolved oxygen optode sensors used on Spray gliders in the CCS, the drift over 5 years since calibration is quantified. The drift can be described well with an exponential model. The observed 100-day deployment drift is larger than the 100-day storage drift, suggesting that the drift rate may depend on intensity of usage. The suggested procedure for two-point calibrations of the optode sensors is an in-water calibration at full saturation and a measurement at zero-oxygen using a sodium sulfite solution. Gain coefficients after 5 years approached 8%, highlighting the need for periodic corrections. The uncertainty of the correction procedure is the larger of 0.5% (0.9% including outliers) or 0.5 μmol kg^{-1} (0.011 mL L^{-1}), depending on oxygen concentration. The correction procedure addresses the drift in the oxygen optode over time, one of the major sources of error. As global ocean deoxygenation is of concern as an impact of climate change, calibrated dissolved oxygen optode sensors are of utmost importance to observing changes in the oceans with accuracy. A simple, in-house two-point calibration can be done close in time to deployment and recovery to determine whether drift of an oxygen optode occurred during storage or deployment.

Acknowledgments. We gratefully acknowledge the support of the National Oceanographic and Atmospheric Administration Global Ocean Monitoring and Observation Program (NA20OAR4320278) and Integrated Ocean Observing System (NA21NOS0120088). A.S.R. was supported by the DOD NDSEG fellowship and the Postdoctoral Scholar Program at Woods Hole Oceanographic Institution, with funding provided by the Doherty Foundation. The Instrument Development Group at Scripps Institution of Oceanography is responsible for operations of Spray gliders in the CUGN. In particular, we thank Jeff Sherman, Ben Reineman, Evan Goodwin, Derek Vana, and Kyle Grindley. We thank three anonymous reviewers for comments that greatly improved the manuscript.

Data availability statement. The data generated in the study are available in the SEANOE online data repository at https://doi.org/10.17882/93431 via a CC BY-NC-ND license (Ren and Rudnick 2023).

REFERENCES

Aanderaa, 2015: TD 269 operating manual oxygen optode 4330, 4831, 4835. Aanderaa Data Instruments Doc., 93 pp., https://www.aanderaa.com/media/pdfs/oxygen-optode-4330-4835-and-4831.pdf.

Alkire, M. B., C. Lee, E. D'Asaro, M. J. Perry, N. Briggs, I. Cetinić, and A. Gray, 2014: Net community production and export from Seaglider measurements in the North Atlantic after the spring bloom. *J. Geophys. Res. Oceans*, **119**, 6121–6139, https://doi.org/10.1002/2014JC010105.

Benson, B. B., and D. Krause Jr., 1984: The concentration and isotopic fractionation of oxygen dissolved in freshwater and seawater in equilibrium with the atmosphere. *Limnol. Oceanogr.*, **29**, 620–632, https://doi.org/10.4319/lo.1984.29.3.0620.

Bittig, H. C., and A. Körtzinger, 2015: Tackling oxygen optode drift: Near-surface and in-air oxygen optode measurements on a float provide an accurate in situ reference. *J. Atmos. Oceanic Technol.*, **32**, 1536–1543, https://doi.org/10.1175/JTECH-D-14-00162.1.

——, B. Fiedler, T. Steinhoff, and A. Körtzinger, 2012: A novel electrochemical calibration setup for oxygen sensors and its use for the stability assessment of Aanderaa optodes. *Limnol. Oceanogr. Methods*, **10**, 921–933, https://doi.org/10.4319/lom.2012.10.921.

——, and Coauthors, 2018a: Oxygen optode sensors: Principle, characterization, calibration, and application in the ocean. *Front. Mar. Sci.*, **4**, 429, https://doi.org/10.3389/fmars.2017.00429.

——, and Coauthors, 2018b: Quality control procedures for oxygen and other biogeochemical sensors on floats and gliders. Recommendations on the conversion between oxygen quantities for Bio-Argo floats and other autonomous sensor platforms. SCOR Tech. Rep. SCOR WG 142, 6 pp., https://archimer.ifremer.fr/doc/00348/45915/.

——, and Coauthors, 2019: A BGC-Argo guide: Planning, deployment, data handling and usage. *Front. Mar. Sci.*, **6**, 502, https://doi.org/10.3389/fmars.2019.00502.

Bushinsky, S. M., S. R. Emerson, S. C. Riser, and D. D. Swift, 2016: Accurate oxygen measurements on modified Argo floats using in situ air calibrations. *Limnol. Oceanogr. Methods*, **14**, 491–505, https://doi.org/10.1002/lom3.10107.

Culberson, C. H., G. P. Knapp, M. C. Stalcup, R. T. Williams, and F. Zemlyak, 1991: A comparison of methods for the determination of dissolved oxygen in seawater. WOCE Rep. 73/91, 83 pp., https://hdl.handle.net/1912/243.

Damerell, G. M., K. J. Heywood, A. F. Thompson, U. Binetti, and J. Kaiser, 2016: The vertical structure of upper ocean variability at the Porcupine Abyssal Plain during 2012–2013. *J. Geophys. Res. Oceans*, **121**, 3075–3089, https://doi.org/10.1002/2015JC011423.

D'Asaro, E. A., and C. McNeil, 2013: Calibration and stability of oxygen sensors on autonomous floats. *J. Atmos. Oceanic Technol.*, **30**, 1896–1906, https://doi.org/10.1175/JTECH-D-12-00222.1.

Demas, J. N., B. A. DeGraff, and P. B. Coleman, 1999: Peer reviewed: Oxygen sensors based on luminescence quenching. *Anal. Chem.*, **71**, 793A–800A, https://doi.org/10.1021/ac9908546.

Garcia, H. E., and L. I. Gordon, 1992: Oxygen solubility in seawater: Better fitting equations. *Limnol. Oceanogr.*, **37**, 1307–1312, https://doi.org/10.4319/lo.1992.37.6.1307.

Haskell, W. Z., II, D. E. Hammond, M. G. Prokopenko, E. N. Teel, B. N. Seegers, M. A. Ragan, N. Rollins, and B. H. Jones, 2019: Net community production in a productive coastal ocean from an autonomous buoyancy-driven glider. *J. Geophys. Res. Oceans*, **124**, 4188–4207, https://doi.org/10.1029/2019JC015048.

Howatt, T., J. B. Palter, J. B. R. Matthews, B. deYoung, R. Bachmayer, and B. Claus, 2018: Ekman and eddy exchange of freshwater and oxygen across the Labrador shelf break. *J. Phys. Oceanogr.*, **48**, 1015–1031, https://doi.org/10.1175/JPO-D-17-0148.1.

Hull, T., N. Greenwood, A. Birchill, A. Beaton, M. Palmer, and J. Kaiser, 2021: Simultaneous assessment of oxygen- and nitrate-based net community production in a temperate shelf sea from a single ocean glider. *Biogeosciences*, **18**, 6167–6180, https://doi.org/10.5194/bg-18-6167-2021.

Johnson, K. S., J. N. Plant, S. C. Riser, and D. Gilbert, 2015: Air oxygen calibration of oxygen optodes on a profiling float array. *J. Atmos. Oceanic Technol.*, **32**, 2160–2172, https://doi.org/10.1175/JTECH-D-15-0101.1.

Körtzinger, A., J. Schimanski, and U. Send, 2005: High quality oxygen measurements from profiling floats: A promising new technique. *J. Atmos. Oceanic Technol.*, **22**, 302–308, https://doi.org/10.1175/JTECH1701.1.

Langdon, C., 2010: Determination of dissolved oxygen in seawater by Winkler titration using the amperometric technique. The GO-SHIP repeat hydrography manual: A collection of expert reports and guidelines, IOCCP Rep. 14, https://doi.org/10.25607/OBP-1350.

Nicholson, D. P., and M. L. Feen, 2017: Air calibration of an oxygen optode on an underwater glider. *Limnol. Oceanogr. Methods*, **15**, 495–502, https://doi.org/10.1002/lom3.10177.

——, S. Emerson, and C. C. Eriksen, 2008: Net community production in the deep euphotic zone of the subtropical North Pacific Gyre from glider surveys. *Limnol. Oceanogr.*, **53**, 2226–2236, https://doi.org/10.4319/lo.2008.53.5_part_2.2226.

——, S. T. Wilson, S. C. Doney, and D. M. Karl, 2015: Quantifying subtropical North Pacific Gyre mixed layer primary productivity from Seaglider observations of diel oxygen cycles. *Geophys. Res. Lett.*, **42**, 4032–4039, https://doi.org/10.1002/2015GL063065.

Pelland, N. A., C. C. Eriksen, S. R. Emerson, and M. F. Cronin, 2018: Seaglider surveys at Ocean Station Papa: Oxygen kinematics and upper-ocean metabolism. *J. Geophys. Res. Oceans*, **123**, 6408–6427, https://doi.org/10.1029/2018JC014091.

Pietri, A., and J. Karstensen, 2018: Dynamical characterization of a low oxygen submesoscale coherent vortex in the eastern North Atlantic Ocean. *J. Geophys. Res. Oceans*, **123**, 2049–2065, https://doi.org/10.1002/2017JC013177.

Pizarro, O., N. Ramírez, M. I. Castillo, U. Cifuentes, W. Rojas, and M. Pizarro-Koch, 2016: Underwater glider observations in the oxygen minimum zone off central Chile. *Bull. Amer. Meteor. Soc.*, **97**, 1783–1789, https://doi.org/10.1175/BAMS-D-14-00040.1.

Ren, A. S., and D. L. Rudnick, 2023: Data to determine drift characteristics of Sea-Bird dissolved oxygen optode sensors. SEANOE, accessed 3 May 2023, https://www.seanoe.org/data/00822/93431/.

Roemmich, D., and Coauthors, 2009: The Argo program: Observing the global ocean with profiling floats. *Oceanography*, **22** (2), 34–43, https://doi.org/10.5670/oceanog.2009.36.

Rudnick, D. L., 2016: Ocean research enabled by underwater gliders. *Annu. Rev. Mar. Sci.*, **8**, 519–541, https://doi.org/10.1146/annurev-marine-122414-033913.

——, K. D. Zaba, R. E. Todd, and R. E. Davis, 2017: A climatology of the California Current System from a network of

underwater gliders. *Prog. Oceanogr.*, **154**, 64–106, https://doi.org/10.1016/j.pocean.2017.03.002.

Schütte, F., J. Karstensen, G. Krahmann, H. Hauss, B. Fiedler, P. Brandt, M. Visbeck, and A. Körtzinger, 2016: Characterization of "dead-zone" eddies in the eastern tropical North Atlantic. *Biogeosciences*, **13**, 5865–5881, https://doi.org/10.5194/bg-13-5865-2016.

Sea-Bird, 2017: User manual: SBE 63 optical dissolved oxygen sensor with RS-232 interface. Sea-Bird Doc., 59 pp., https://www.seabird.com/asset-get.download.jsa?code=251379.

Sherman, J., R. E. Davis, W. B. Owens, and J. Valdes, 2001: The autonomous underwater glider "Spray." *IEEE J. Oceanic Eng.*, **26**, 437–446, https://doi.org/10.1109/48.972076.

Uchida, H., T. Kawano, I. Kaneko, and M. Fukasawa, 2008: In situ calibration of optode-based oxygen sensors. *J. Atmos. Oceanic Technol.*, **25**, 2271–2281, https://doi.org/10.1175/2008JTECHO549.1.

Weiss, R. F., and B. A. Price, 1980: Nitrous oxide solubility in water and seawater. *Mar. Chem.*, **8**, 347–359, https://doi.org/10.1016/0304-4203(80)90024-9.